

Assessment of Acid Mine Drainage's Impact on Makhat's Watershed Plants (Taza Province, Morocco)

Ikram Lahmidi^{1*}, Narmine Assabar¹, Laila Mesrar^{1,2}, Marouane Laaraj³, Raouf Jabrane¹

¹ Laboratory of Intelligent System, Georesources and Renewable Energies, Faculty of Science and Technology of Fez, Morocco

² LOMC UMR 6294 CNRS, University Le Havre Normandie, 76600 Le Havre, France

³ Laboratory of Functional Ecology and Environment Engineering, University of Sidi Mohammed Ben Abdellah, FST Fes, Route d'Imouzzer P.O. Box: 2202, 30 000 Morocco

* Corresponding author's e-mail: ikram.lahmidi@usmba.ac.ma

ABSTRACT

The mining production industry often leaves large quantities of mine spoil heaps exposed on the surface. The lack of monitoring of these discharges could create sources of pollution; the most common among them is acid mine drainage, which causes the contamination of the environment by heavy metals present in its solutions. Bouaazza's mine, present in Taza province North-East Morocco, was known for lead and sulfide exploitation for many years, which contributed to the exposure of important quantities of acid spoil heaps on the surface. To assess the impact caused by acid mine drainage in Makhat's stream plants, sediments, and plant samples were collected along the stream. Physicochemical results for sediments showed pH values below 6. Geochemical results for sediments indicated Pb concentrations higher than the World Surface Rock Average standards (16 ppm), with values over 3000 ppm. As for plants, the values found after ICP-AES analyses were higher than the WHO permissible limit (2 ppm). These results confirm the harmful impact of the lack of environmental monitoring while and after abandoning mining explorations, which leads to environmental disasters.

Keywords: acid mine drainage, Bouaazza's mine, pollution, plants, sediments, Makhat's stream.

INTRODUCTION

In recent times, and with the development of many sectors in several countries all over the world, anthropogenic activities produce a huge amount of organic and inorganic substances into the environment, which causes negative impact on the environment that eventually, threaten animal and human health [Siddiqua et al., 2022; Hama Aziz et al., 2023]. Industries in particular deliver a massive number of composites into the environment generally associated with wastewater ejections that have significant negative influences [Katheresan et al., 2018]. Although the economic development related to the mining sector in many countries, specifically represents a continuous pollution generator, indicating the

primary source of heavy metal contamination during the exploitation and for many decades after the mining activity is finished in the mining area [Swain, 2024]. One of the main forms of this pollution is acid mine drainage.

In the last 20 years, many researchers all over the world have shown huge interest in the negative impacts on the environment generated by acid mine drainage. Usually, natural parameters initiate the processes of AMD in the environment but this process can be aggravated due to mining activities. Consequently, acid mine drainage arises from the fast oxidation of sulfide minerals present in the embankments; this oxidation happens when these minerals are exposed to the atmosphere [Ojonimi et al., 2019]. AMD is extensively spread and has serious consequences on

the environment, and the majority of mining countries deal with environmental problems related to it. In the United States, acid mine drainage caused many environmental disasters; more than 8000–16000 km of rivers were polluted in the western part of the US, while coal mines polluted more than 6000 km of rivers in the eastern part due to AMD according to the US Forest Service. In Australia, more than 21,500 km² of land was damaged from mining activities [Naidu et al., 2019].

Morocco is a mining country by excellence thanks to the mineral resources present in abundance in the country. However, mining discharges left from the exploitations of minerals represent heavy topics attracting researchers to highlight their negative impacts on fauna and flora [Lghoul et al., 2014; Lakrim et al., 2016; Ech-charef et al., 2023]. Ait Amar mining area's soils results for example showed relatively acidic pH and high organic carbon content (1.06–5.01%), while Zn, Cr and Fe values were exceeding some European soil standards with very high levels of Fe (about 435 500 ppm) and P (9200 ppm), and slightly high Cr and Zn contents (222.16 ppm and 153.3 ppm respectively) due to acid mine drainage [Nouri et al., 2013]. The impact is present too in Kettara 35 km northwest of Marrakech city, which is a past underground mine that operated for 44 years (1938–1982), and was since 1964 mainly used to produce sulfuric acid that led to the production of approximately 3 million tons of sulfur-rich mining waste dumped over an area of 16 ha [Boularbah et al., 1996; Babi et al., 2016].

Taza province in Morocco has known many exploration activities thanks to its geographical location and geological history, these activities revealed the presence of mines such as galena, dolomite, and calcite. The exploitation of these mines left huge amounts of mining discharges directly exposed to the environment. Studies highlighted this pollution in Taza province, which is found in Ain Aouda's soils results that confirmed the pollution of soils by lead, copper, zinc and arsenic due to the mine's spoil heaps with maximum concentration reaching 495.750 (ppm), 328.65 (ppm), 19858.800 (ppm), and 1280.700 (ppm) respectively [As-sabar et al., 2023 a; 2023 b].

The mine of Bouaazza present in Taza province and the middle of Makhat's stream has experienced some intense activities generating an important area rich in acidic tailings. The degree

of this pollution can be confirmed by the results found largely exceeding national and international limits for pH values that were below 4 for surface water, and Pb values that were more than 300 ppm in the soils [Lahmidi et al., 2023].

This study aims to evaluate the impact of acid mine drainage on the plants in Makhat's stream. To achieve this, concentrations of Cu, Ni, Zn, and Pb in the plants were estimated, and the physico-chemical factors and heavy metal values of the surrounding sediments were analyzed and calculated. These data were then used to estimate the bioaccumulation factor.

MATERIALS AND METHODS

Study area

The Dar Bouaazza deposit is located in the South-West part of the city of Taza [Laaraj et al., 2020; 2022; 2024] in the mountainous area of Tazekka in the North Eastern part of Morocco. The deposit could be reached by taking the national Taza-Fez road from Taza city for a distance of approximately 12 km, then a 6 km runway joining Bab Merzoukka's small town to the deposit. The mine is located in the Paleozoic buttonhole of Tazekka with some outcrops of the granitic basement, and its borders are formed by very old secondary formations. The NE-SW main veins of the deposit are found in the lower Ordovician epimetamorphic shales of Tazekka [Hoepffner, 1987]. The sub-vertical veins among shales mostly have galena mineralization associated with chalcopyrite, quartz, pyrite, and sphalerite. The embankments caused by the previous exploitations of the mine are positioned on the eastern slopes of the river of Makhat.

The Tazekka massif shows a humid environment in a dry region. Its main particularity remains in gathering 6 major forest species of Morocco in a small space: the Atlas cedar (*Cedrus atlantica*), the Zen oak (*Quercus faginea*), the cork oak (*Quercus suber*), the holm oak (*Quercus rotundifolia*), Kermes oak (*Quercus coccifera*), and Thuja (*Tetraclinis articulata*), therefore it presents an original and rich phyto-diversity, of which 64 taxa are strictly endemic [Fougrach et al., 2007] resulted from its geographical position, orography, edaphic structure, and past and current climatic conditions.

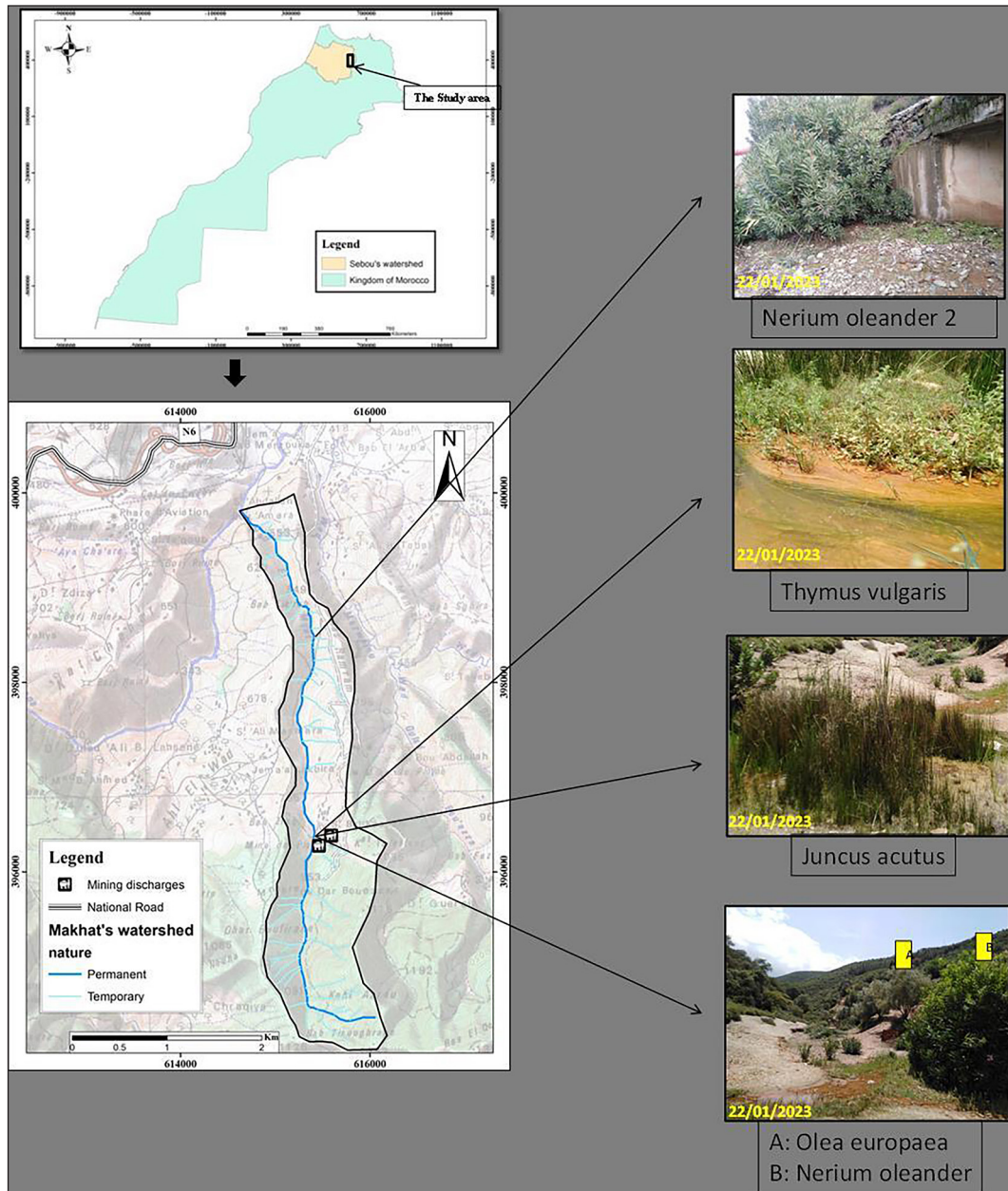


Figure 1. Sampling sites and Makhat's watershed position

Sampling and analyses

Figure 1 represents the placement of the six samples of plants that were collected from 2 sites in Makhat's stream in January 2023. The first five samples represent the first site, they were collected near the mining discharges area; they represent Oleander (*Nerium oleander*), Pistachio mastic tree (*Pistacia lentiscus*), Spiny rush (*Juncus acutus*), Olive tree (*Olea europaea*) and Thyme (*Thymus vulgaris*). Meanwhile, the sixth sample refers to another sample of Oleander (*Nerium oleander* 2) which was taken from site 2 almost two kilometers far from the mining site to evaluate heavy

metals concentrations between the two samples in different environments. The shoot and the root parts of each sample were collected separately to have an exact answer on the distribution and location of heavy metal accumulation in each plant. Each part of the plant was put in a labeled polyethylene plastic bag and then transported to the laboratory in a cooler where they were stored in a freezer at low temperature to restrict sample degradation and loss of pollutants to preserve their condition until the analysis.

Three sediment samples were taken from Makhat's stream, two from the first sampling site where one of them was near *Pistacia lentiscus* and

the other was near the rest of the plant from the first sampling site, while the last sediment sample was obtained from site 2 near Nerium oleander 2. Sediment samples were stored in labeled polyethylene bags with a thickness of 50 µm and then sent to the laboratory where they were dried at 60 °C and sieved through a 2 mm sieve to prepare them for the following physicochemical analyses: The percent of total organic matter in samples by loss on ignition (LOI) [Norme NF ISO 14235, 1998], electrical conductivity (EC), water pH [Norme NF ISO X 31-301, 1989] and the residual humidity [Norme NF ISO 11465, 1994]. Cooper (Cu), nickel (Ni), zinc (Zn), and lead (Pb) for sediment samples were estimated by the inductively coupled plasma atomic emission spectroscopy (ICP-AES) after bringing all the solid phases into solution without any residue remaining using the triacid attack [Norme NF X 31-147, 1996].

For plant samples, the calculation of heavy metal concentrations was possible after the mineralization of samples into liquid phases following the protocol described by J. Lambert (1975) [Lambert, 1997]. This step allows the calculation of Cu, Ni, Zn, and Pb values by ICP-AES in plants' parts of the study area.

All the heavy metal concentrations of sediments and plants for ICP-AES were analyzed at the University of Sidi Mohamed Ben Abdellah's Laboratory of the Innovation City Fez, Morocco.

Bioaccumulation factor (BAF)

Metals are conservative pollutants. Therefore, the accumulation of metals by plants depends on the metal and the organism. Some organisms have only a limited ability to regulate metal concentration; others are not able to easily excrete some specific metals (such as Cd and Hg) and as a result, the concentration in the tissues of organisms increases over time, leading to bioaccumulation [Sumalan et al., 2023; Skuza et al., 2022]. Bioaccumulation is often a good indicator of the exposure of organisms to certain chemical compounds present in contaminated ecosystems

and can be measured using the bioaccumulation factor (BAF) [Savoca and Pace, 2021]. The bioaccumulation factors represent the proportion between the element concentrations in the emerging plant material in comparison with the element total concentration in the sediment. The BAF for each specific element was calculated using the following Formula 1:

$$BAF = \frac{[Heavy\ metal\ concentration\ in\ the\ plant]}{[Heavy\ metal\ concentration\ in\ the\ sediment]} \quad (1)$$

Translocation factor

The translocation factor (TF) is expressed by the concentration of a translocated element in the aerial biomass on the concentration remaining in the biomass root. Indeed, it is well known that roots play an important role in exclusion mechanisms through the storage of heavy metals [Baker, 1981]. A significant proportion of these elements therefore may have been stabilized in the root systems of plants. The estimation of the translocation factor for each heavy metal is possible by applying the following Equation 2:

$$TF = \frac{[Heavy\ metal\ concentration\ in\ plant\ shoot\ (mg/Kg)]}{[Heavy\ metal\ concentration\ in\ plant\ root\ (mg/Kg)]} \quad (2)$$

RESULTS

Sediments' physicochemical factors and heavy metals concentrations

Table 1 summarizes the results of the physicochemical properties found in the sediments near Makhat's river's plants. The weight loss method was used to measure sediments' humidity; the percent of the mass of water found is the result of the difference in weight before and after evaporation [Baalousha et al. 2022]. Moisture measurement results showed that the values obtained range from 4.39 to 14.5% which could be explained by the different texture and granulometric composition of the sediments of Makhat's river.

The aptitude to reduce differences in acidity or alkalinity of mining discharges in their

Table 1. The sediments of Makhat's river physicochemical factors

Samples	Humidity (%)	pH	EC (µs/cm)	LOI (%)
S1	14.5	5.15	826	15.93
S2	5.92	5.6	773	1.98
S3	4.39	6.41	152	2.36

environment area is highly connected to their composition of organic matter; this later influences the mobilization and disposal of heavy metals in the sediment that form organometallic compounds following their interaction with organic matter [Fashola et al., 2016]. LOI values calculated range from 1.98 to 15.93%, indicating that the S1 sample has the highest percentage of organic matter.

The results indicated that the pH of the sediment varies between 5.15 and 6.41. Acidic values were found in the S1 and S2 sediment samples, which are located near the mining area, whereas the S3 sample, situated farther downstream, showed slightly acidic values, explaining its higher pH. However, the electrical conductivity in all samples was very low, with the highest value being 826 $\mu\text{S}/\text{cm}$, observed in the S1 sample. The results of heavy metals values for Makhat's sediments, detailed in Table 2, indicate that Ni concentrations in all samples are below the World Surface Rock Average. This is also true for Cu and Zn in the S3 sample. However, Pb values in the S1 and S2 samples, located near the mining area, exceed admissible standards by 230 and 100 times, respectively. These concentrations tend to decrease remarkably further downstream in Makhat's river.

The principal component analysis (PCA) was applied to better understand the link between the physicochemical factors and heavy metals in Makhat's sediments; the results of this approach are presented in Table 3 and Figure 2. Table 3 shows the results of the matrix of correlation coefficients between Makhat's sediments' physicochemical factors and heavy. The values calculated show some strong positive and negative correlations between some sets: very high positive correlations were found between (EC, Cu), (EC, Pb), (EC, Zn), (Ni, Cu) and (Pb, Zn), however high negative correlations were obtained between (pH, EC), (pH, Pb), (pH, Zn), (LOI, EC), (LOI, Cu) and (LOI, Ni). The results of strong correlations support the theory of the link between the electrical conductivity and some heavy metals in the

sediments, and between lead and zinc, which indicates the dependency between some pairs.

Figure 2a results indicate that the F1 axis covers the majority of the total information (82%), while F2 only covers 18% of the total information. However, the factorial plane of F1-F2 exposes the whole total inertia (100%), thus all the information from the PCA results analysis is represented in these axes; they indicate a good representation and distribution of the investigated factors. Axis F1 gathers the majority of heavy metals and the electrical conductivity with positive correlations; these dispositions confirm the results obtained in Table 3 of the matrix of correlation; on the other hand, pH and LOI were placed on the side of negative correlation. However, Ni was placed in the middle of F1 and F2, which explains 18% of the total information found for the F2 axis.

Figure 2b shows the position of the three samples on the map; it indicates the presence of 3 diverse positions: The first position includes the S1 sample collected near the mine characterized by high concentrations of Pb and Zn which explains its position in the map in the side of high correlations of Pb, EC and Zn. The second position is represented by the S2 sample that has very high values of Cu and Ni explaining its location on the same side of their correlations. The last location is for the S3 sample that had low concentrations of heavy metals and had slightly acidic pH values which indicates its location in the same position of pH correlation.

Plants heavy metals concentrations

Figure 3 shows the results found for heavy metals in Makhat's river plants in comparison with WHO permissible limits. All the sample concentrations were under the permissible limit (10 ppm) for Cu (a) and Ni (c) except for Pistacia lentiscus which had values 1.7 times higher than the permissible limit for Ni. Pb results (d) calculated range from 13 to 29 ppm; they are 6.8, 7.3, 7.7, 9.4, and 14.3 times higher than the

Table 2. The sediments of Makhat's river heavy metals concentrations (ppm)

Samples	Cu	Ni	Pb	Zn
S1	143	18.51	3668	622
S2	255	34.83	1577	498
S3	6.036	9.39	32.43	54.38
World surface rock average (Martin and Meybeck, 1979)	32	49	16	127

Table 3. Matrix of correlation coefficients between Makhat’s sediments physicochemical factors and heavy metals

Variables	pH	EC (μs/cm)	LOI (%)	Cu	Ni	Pb	Zn
pH	1	-0.958	0.715	-0.678	-0.501	-0.969	-0.989
EC (μs/cm)	-0.958	1	-0.885	0.859	0.727	0.858	0.990
LOI (%)	0.715	-0.885	1	-0.999	-0.963	-0.520	-0.812
Cu	-0.678	0.859	-0.999	1	0.976	0.475	0.781
Ni	-0.501	0.727	-0.963	0.976	1	0.272	0.626
Pb	-0.969	0.858	-0.520	0.475	0.272	1	0.921
Zn	-0.989	0.990	-0.812	0.781	0.626	0.921	1

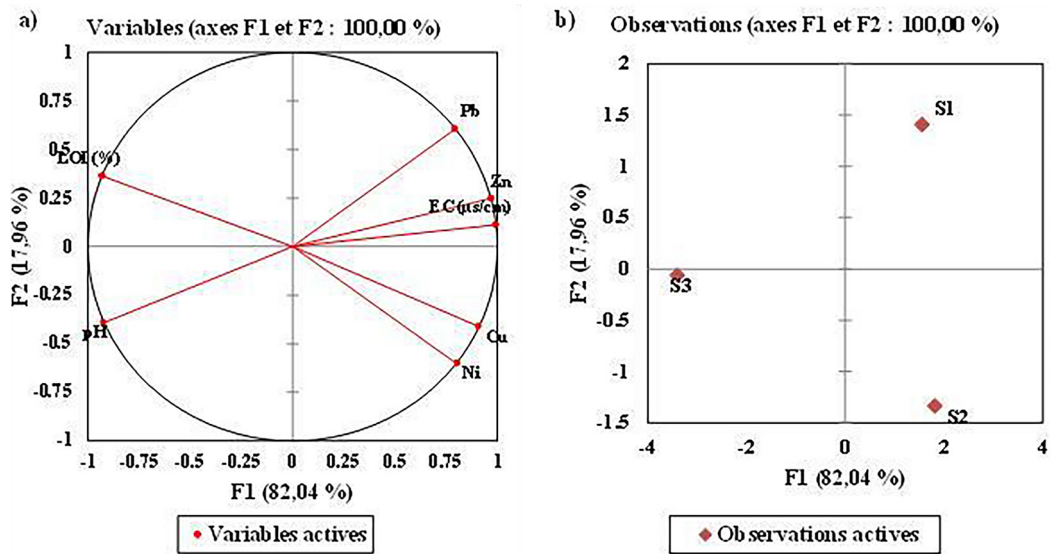


Figure 2. (a) Physicochemical factors and heavy metals correlation circle analyzed in sediments samples, (b) samples sites correlation map

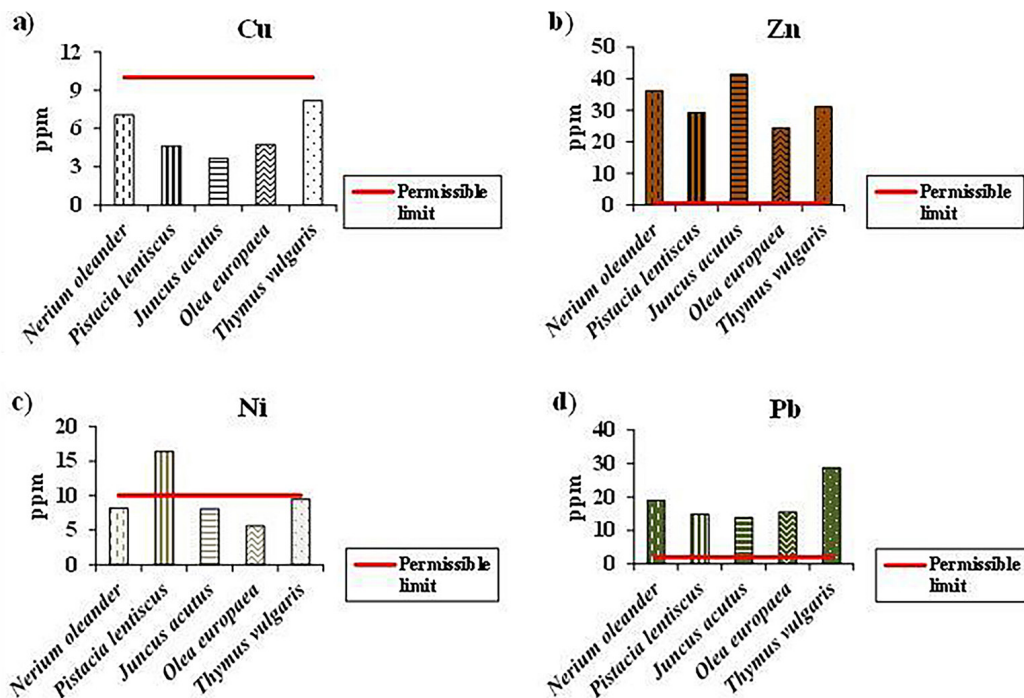


Figure 3. Heavy metals concentrations of Makhat’s stream plants

permissible limit (2 ppm) for *Juncus acutus*, *Pistacia lentiscus*, *Olea europaea*, *Nerium Oleander*, and *Thymus vulgaris* respectively. Zn values (b) were also over the permissible limit for all the samples; the concentrations were 69 times higher for *Juncus acutus*, 60 times for *Nerium oleander*, 52 times for *Thymus vulgaris*, 49 times for *Pistacia lentiscus* and 41 times for *Olea europaea*. Figure 2 further demonstrates the absorption capacity of each plant for specific elements. *Thymus vulgaris* showed the highest concentrations of Cu and Pb, *Juncus acutus* exhibited peak Zn levels, while *Pistacia lentiscus* absorbed the maximum Ni concentrations.

The values of the correlation matrix of Makhat’s plants, shown in Table 4, indicates a strong positive correlation only between Cu and Pb. None of the other element pairs showed strong positive or negative correlations. The result of the strong positive correlation between Cu and Pb supports the theory of a link between these two elements, indicating a significant dependency between them in the plants’ heavy metal uptake.

The principal component analysis results (Figure 4a) shows that the F1 axis accounts for 49% of the total variance, while the F2 axis accounts for 27%. Together, the F1-F2 factorial plane gathers almost 76% of the total inertia, making them sufficient to represent the PCA analysis results and effectively demonstrate the

distribution and representation of heavy metals in Makhat’s stream plants. Cu and Pb show a strong positive correlation on the F1 axis. In contrast, the F2 shows Ni with a positive correlation and Zn with a negative correlation. These results support the strong correlation between Cu and Pb found in the matrix of correlation.

Figure 4b shows the location of plant samples on the correlation map, identifying the presence of four distinct categories. The first category includes the *Thymus vulgaris* sample, situated near the Pb and Cu side due to its high concentrations of these elements. The second group is represented by *Pistacia lentiscus* and *Olea europaea* samples. The heavy metals present in *Pistacia lentiscus* show very high concentrations of Ni, aligning with its position on the same side as the Ni correlation, while *Olea europaea*, with the lowest Ni values, is located on the side corresponding to low Ni levels. The third group includes the *Juncus acutus* sample, positioned on the same side as Zn on the correlation map, corroborating ICP results that indicated *Juncus acutus* had the highest Zn values. The final category is represented by *Nerium oleander*, situated near Pb and Cu, reflecting its high concentrations of these elements.

Figure 5 compares two samples of *Nerium oleander*: one collected near the mine and the other downstream. The results show that the concentrations of Ni, Cu, Pb, and Zn in the downstream

Table 4. Matrix of correlation coefficients of Makhat’s plants heavy metals

Variables	Cu	Ni	Pb	Zn
Cu	1	-0.082	0.918	-0.109
Ni	-0.082	1	-0.075	-0.072
Pb	0.918	-0.075	1	-0.111
Zn	-0.109	-0.072	-0.111	1

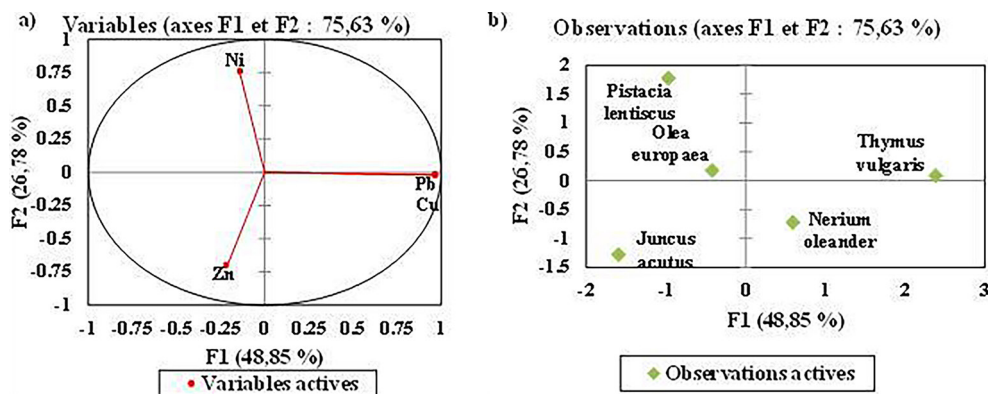


Figure 4. (a) Heavy metals correlation circle analyzed in plants’ samples, (b) Plants sites correlation map

sample were 57%, 48%, 35%, and 20% lower, respectively, than those in the sample collected near the mining site. This explains that the impact of Bouaazza’s embankments decreases with distance from the mining area.

DISCUSSIONS

The long exposure of plants and aquatic systems to damaging and toxic heavy metals such as Ni, Cu, Zn and Pb present in the embankments near mining areas can cause significant impacts on the environmental health [Singh and Kalamdhad, 2011]. To understand the impact of historical mining activities in the area, physicochemical and geochemical parameters were assessed for the sediments and plants of Makhat’s stream. The sediment pH calculated ranged from 5.15 to 6.41. The slightly acidic value of the S3 sample, located far from the mining site, resulted in higher pH values compared to the more acidic S1 and S2 samples situated near Bouaazza’s embankments. These results are similar to the ones found in several Colorado AMD-impacted streams that had acidic pH values ranging from 2.60 to 4.54 [Baeseman et al., 2006]. ICP- AES analysis of heavy metals in the sediments of Makhat’s stream showed Pb values of 3668 and 1577 ppm in the S1 and S2 samples, respectively, located near the mining area. These values are 230 and 100 times higher

than the permissible limits, proving the significant impact of Bouaazza’s spoil heaps on Makhat’s sediments. Similarly, Cu and Zn values in the S1 and S2 samples exceeded the standard levels. These results are similar to the conclusions found in Ngwenya, Swaziland, that showed percent mean levels of all heavy metals in the bioavailable fractions in the Quarry Dam sediment samples higher than WHO standards [Dalmini et al., 2013].

Compared to the WHO standards, Pb values ranged from 13 to 29 ppm, significantly exceeding the permissible limit of 2 ppm by values of 6.8, 7.3, 7.7, 9.4, and 14.3 in *Juncus acutus*, *Pistacia lentiscus*, *Olea europaea*, *Nerium oleander*, and *Thymus vulgaris* respectively. All samples had Cu and Ni concentrations below the permissible limit of 10 ppm, except for *Pistacia lentiscus*, which had Ni values 1.7 times higher than the permissible limit. Zn concentrations in all samples also exceeded the permissible limit, being 69 times higher in *Juncus acutus*, 60 times in *Nerium oleander*, 52 times in *Thymus vulgaris*, 49 times in *Pistacia lentiscus*, and 41 times in *Olea europaea*. These results are similar to the heavy metal concentrations in plants near a Korean Cu-W mine, where the average Cu concentrations in plants grown in the mining area ranged from 8.95 to 26.4 $\mu\text{g}\cdot\text{g}^{-1}$ (DW) in corn grain in spring onion surpassing the required limit for Cu (5 to 20 $\mu\text{g}\cdot\text{g}^{-1}$ (DW)). Similarly, Pb concentrations in

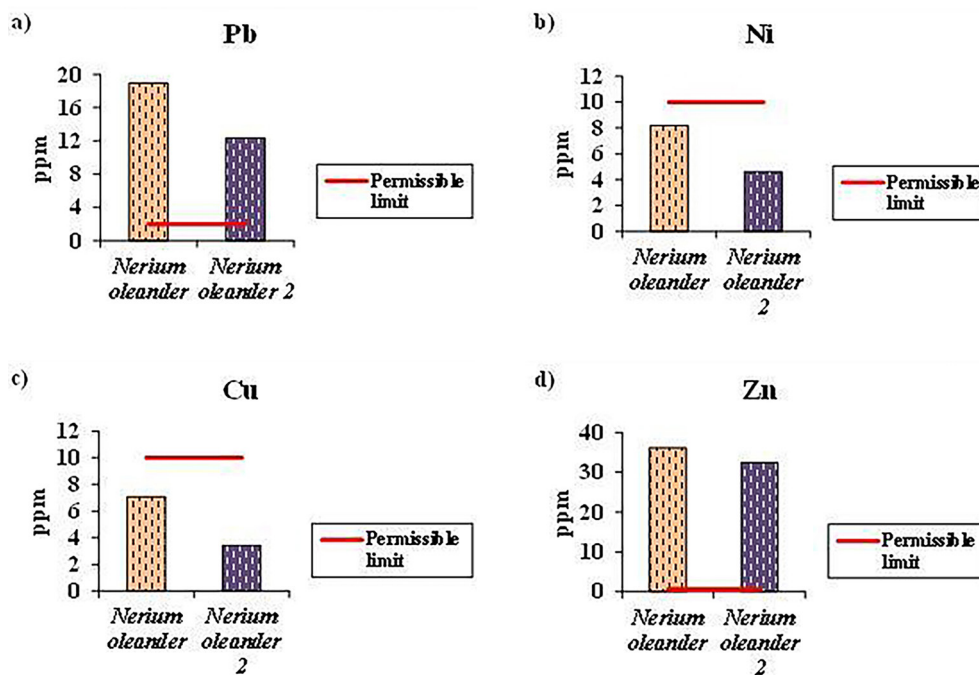


Figure 5. The comparison of heavy metals concentrations of *Nerium oleander* samples

spring onions were $4.23 \mu\text{g}\cdot\text{g}^{-1}$ (DW), exceeding the normal range for plants (0.01 to $3.85 \mu\text{g}\cdot\text{g}^{-1}$ (DW)) [Jung, 2008]. The results confirmed the negative impacts generated by acid mine drainage on Makhat's stream plants.

CONCLUSIONS

To comprehensively assess the negative effects of acid mine drainage (AMD) resulting from historical mining activities (discharges) at Bouaazza's deposit on the vegetation in Makhat's stream, the physicochemical factors of the sediments near the plant's samples were analyzed. The pH of the sediment samples ranged from 5.15 to 6.41. The slightly acidic pH value of 6.41 in the S3 sample is attributed to its distance away from the mining site. In contrast, the S1 and S2 sediment samples exhibited more acidic pH values due to their proximity to Bouaazza's embankments. The values of moisture measurements analyzed showed results from 4.39 to 14.5 %, likely influenced by the varied texture and granulometric composition of Makhat's sediments. Analysis of heavy metals in Makhat's sediments via ICP-AES showed Ni concentrations below the World Surface Rock Average standards in all the samples. However, Pb values exceeded admissible standards by 230 and 100 times for the S1 and S2 samples from the mining area, reaching 3668 and 1577 ppm, respectively, confirming the significant impact of Bouaazza's spoil heaps on Makhat's sediments.

Compared to WHO standards, only the *Pistacia lentiscus* sample had values 1.7 times higher than the permissible limit for Ni; the other samples remained below the limit (10 ppm) for Cu and Ni. However, Pb concentrations exceeded the permissible limit in all samples, ranging from 13 to 29 ppm, being 6.8, 7.3, 7.7, 9.4, and 14.3 times higher for *Juncus acutus*, *Pistacia lentiscus*, *Olea europaea*, *Nerium oleander*, and *Thymus vulgaris*, respectively. Zn values also surpassed the limit for all the samples, with concentrations being 69 times higher for *Juncus acutus*, 60 times for *Nerium oleander*, 52 times for *Thymus vulgaris*, 49 times for *Pistacia lentiscus* and 41 times for *Olea europaea*. The correlation map results indicated the presence of four different categories proving the results found in ICP-AES for plants; all the categories for plants had the same position as the highest concentration of heavy metal they had. The comparison between the results found of 2 samples of *Nerium oleander*, present in two different positions

of Makhat's stream showed that *Nerium oleander* 2 present downstream had concentrations of Ni, Cu, Pb, and Zn were 57%, 48%, 35% and 20% respectively fewer than *Nerium oleander* located in mining discharges, confirming the theory of the increased distance from the mining area reduces the impacts of Bouaazza's embankments.

REFERENCES

1. Assabar N., Lahmidi I., Jabrane R. 2023 a. assessment of heavy metals contamination in spoil heaps of ain aouda mine (Taza, Morocco). *J. Ecol. Eng*, 24(3), 224–231. <https://doi.org/10.12911/22998993/157519>
2. Assabar N., Lahmidi I., Choukrad J., Jabrane R. 2023 b. Geochemical characterization of the spoil heaps of the ain aouda mine and its impact on the soil (Morocco). *Ecol. Eng. Environ. Technol*, 24(6), 100–108. doi: doi:10.12912/27197050/168087
3. Baalousha H.M., Ramasomanana F., Fahs M., Seers T.D. 2022. Measuring and validating the actual evaporation and soil moisture dynamic in arid regions under unirrigated land using smart field lysimeters and numerical modeling. *Water*, 14(18), 2787. <https://doi.org/10.3390/w14182787>
4. Babi K., Asselin H., Benzaazoua M. 2016. Stakeholders' perceptions of sustainable mining in Morocco: A case study of the abandoned Ket-tara mine. *Extr. Ind. Soc*, 3(1), 185–192. <https://doi.org/10.1016/j.exis.2015.11.007>
5. Baeseman J.L., Smith R.L., Silverstein J. 2006. Denitrification potential in stream sediments impacted by acid mine drainage: effects of pH, various electron donors, and iron. *Microb Ecol*, 51(2), 232–41. <https://doi.org/10.1007/s00248-005-5155-z>
6. Baker A.J.M. 1981. Accumulators and excluders -strategies in the response of plants to heavy metals. *J. Plant Nutr*, 3, 643–654. <https://doi.org/10.1080/01904168109362867>
7. Boularbah A., Morel J.L., Bitton G., Mench M. 1996. A direct solid-phase assay specific for heavy-metal toxicity. II. Assessment of heavy-metal immobilization in soils and bioavailability to plants. *Soil Sedi- ment Contam*, 5(4), 95–404. <https://doi.org/10.1080/15320389.609383537>
8. Dlamini C.L., Fadiran A.O., Thwala J.M. 2013. A study of environmental assessment of acid mine drainage in Ngwenya, Swaziland. *J. Environ. Prot. (Irvine., Calif)*, 4, 20–26. <https://doi.org/10.4236/jep.2013.411B003>
9. Ech-Charef A., Dekayir A., Jordán G., Rouai M., Chabli A., Qarbous A., El Houfy F.Z. 2023. Soil heavy metal contamination in the vicinity of the abandoned Zeïda mine in the Upper Moulouya Basin, Morocco. Implications for airborne dust pollution under semi-arid

- climatic conditions. *J. African Earth Sci*, 198, 104812. <https://doi.org/10.1016/j.jafrearsci.2022.104812>
10. Fashola M.O., Ngole-Jeme V.M., Babalola O.O. 2016. Heavy metal pollution from gold mines: Environmental effects and bacterial strategies for resistance. *Int J Env. Res Public Heal*, 13(11), 1047. <https://doi.org/10.3390/ijerph13111047>
 11. Fougrach H., Badri W., Malki M. 2007. Flore vasculaire rare et menacée du massif de Tazekka (région de Taza, Maroc). *Bull. l'Institut Sci. Rabat, Sect. Sci. la Vie*, 29, 1–10.
 12. Hama Aziz K.H., Mustafa F.S., Omer K.M., Hama S., Hamarawf R.F., Rahman K.O. 2023. Heavy metal pollution in the aquatic environment: efficient and low-cost removal approaches to eliminate their toxicity: a review. *RSC Adv*, 13(26), 17595–17610. <https://doi.org/10.1039/d3ra00723e>
 13. Hoepffner C. 1987. La tectonique hercynienne dans l'Est du Maroc. University of Strasbourg.
 14. Jung M.C. 2008. Heavy metal concentrations in soils and factors affecting metal uptake by plants in the vicinity of a Korean Cu-W mine. *Sensors (Basel)*, 4, 2413–2423. <https://doi.org/10.3390/s8042413>
 15. Katheresan V., Kansedo J., Lau S.Y. 2018. Efficiency of various recent wastewater dye removal methods: A review. *J. Environ. Chem. Eng*, 6(4), 4676–4697. <https://doi.org/10.1016/j.jece.2018.06.060>
 16. Laaraj M., Benaabidate L., Mesnage V. 2020. Assessment of inaeouene river pollution for potable water supply, Northern Morocco. *J. Ecol. Eng*, 21(7), 68–80. <https://doi.org/10.12911/22998993/125450>
 17. Laaraj M., Mesnage V., Nabih S., Mliyeh M.M., Lahmidi I., Benaabidate L. 2022. Assessment of heavy metals in the sediments of the inaeouene watershed upstream the Idriss 1st Dam, Northern Morocco. *J. Ecol. Eng*, 23(9), 157–170. <https://doi.org/10.12911/22998993/151843>
 18. Laaraj M., Benaabidate L., Mesnage V., Lahmidi I. 2024. Assessment and modeling of surface water quality for drinking and irrigation purposes using water quality indices and GIS techniques in the Inaeouene watershed, Morocco. *Model. Earth Syst. Env*, 10, 2349–2374. <https://doi.org/10.1007/s40808-023-01904-1>
 19. Lahmidi I., Tzoraki O., Mesrar L., Benaabidate L., Assabar N. Laaraj M., Jabrane R. 2023. Assessment of soil and surface water quality in Makhat's Watershed (Taza Province, Morocco). *Ecol. Eng. Environ. Technol*, 24(2), 194–204. <https://doi.org/10.12912/27197050/156972>
 20. Lakrim M., Mesrar L., El Aroussi O., Jabrane R. 2016. Application géomatique pour la cartographie de la vulnérabilité environnementale engendrée par les déchets miniers de la mine ferrifère de Nador (Nord-est du Maroc). *Eur. Sci. Journal, ESJ*, 12(15), 287. <https://doi.org/10.19044/ESJ.2016.V12N15P287>
 21. Lambert J. 1977. Une technique de minéralisation rapide des végétaux en vue du dosage en série de n, p, k, na, ca, mg, fe, etc, note analytique. Lab. d'agriculture - Inst. Natl. Agron. El Harrach – Alger.
 22. Lghoul M., Maqsoud A., Hakkou R., Kchikach A. 2014. Hydrogeochemical behavior around the abandoned Kettara mine site, Morocco. *J. Geochemical Explor*, 144, 456–467. <https://doi.org/10.1016/j.gexplo.2013.12.003>
 23. Naidu G., Ryu S., Thiruvengatchari R., Choi Y., Jeong S., Vigneswaran S.A. 2019. A critical review on remediation, reuse, and resource recovery from acid mine drainage. *Environ. Pollut*, 247, 1110–1124. <https://doi.org/10.1016/j.envpol.2019.01.085>
 24. Nouri M., Gonçalves F., Sousa J.P., Römbke J., Ksibi M., Pereira R., Haddioui A. 2013. Metal concentrations and metal mobility in Ait Am- mar Moroccan mining site. *J. Mater. Environ. Sci*, 5(1), 271–280.
 25. Norme NF ISO 14235. 1998.
 26. Norme NF ISO X31-103. 1988.
 27. Norme NF ISO 11465. 1994.
 28. Norme NF X31-147. 1996.
 29. Ojonimi T.I., Asuke F., Onimisi M.A., Onuh C.Y. 2019. Acid mine drainage (AMD): An environmental concern generated by coal mining. *J. Degrad. Min. LANDS Manag*, 6(4), 1875 – 1881. <https://doi.org/10.15243/jdmlm.2019.064.1875>
 30. Savoca D., and Pace A. 2021. Bioaccumulation, bio-distribution, toxicology and biomonitoring of organo-fluorine compounds in aquatic organisms. *Int J Mol Sc*, 22(12), 6276. <https://doi.org/10.3390/ijms22126276>
 31. Siddiqua A., Hahladakis J.N., Al-Attiya W.A.K.A. 2022. An overview of the environmental pollution and health effects associated with waste landfilling and open dumping. *Env. Sci Pollut Res*, 29, 58514–58536. <https://doi.org/10.1007/s11356-022-21578-z>
 32. Singh J., and Kalamdhad A.S. 2011. Effects of heavy metals on soil, plants, human health and aquatic life. *Int. J. Res. Chem. Environ*, 1(2), 15–21.
 33. Skuza L., Szućko-Kociuba I., Filip E., Bożek I. 2022. Natural molecular mechanisms of plant hyperaccumulation and hypertolerance towards heavy metals. *Int J Mol Sci*, 23(16), 9335. <https://doi.org/10.3390/ijms23169335>
 34. Sumalan R.L., Nescu V., Berbecea A., Sumalan R.M., Crisan M., Negrea P., Ciulca S. 2023. The impact of heavy metal accumulation on some physiological parameters in *Silphium perfoliatum* L. Plants Grown in Hydroponic Systems. *Plants*, 12(8), 1718. <https://doi.org/10.3390/plants12081718>
 35. Swain C.K. 2024. Environmental pollution indices: a review on concentration of heavy metals in air, water, and soil near industrialization and urbanisation. *Discov Env*, 2(5), 1–14. <https://doi.org/10.1007/s44274-024-00030-8>